ISSN 2394-3777 (Print)
ISSN 2394-3785 (Online)
Available online at www.ijartet.com

International Journal of Advanced Research Trends in Engineering and Technology (IJARTET)
Vol. 6, Issue 4, April 2019

Image Processing Methods for 3D Face Recognition

D. Malathi[1], A.Mathangopi[2], Dr. D. Rajini Girinath[3]
P.G Student, Department of CSE, Sri Muthukumaran Institute of Technology, Chennai, India[1]
Asst.Prof, Department of CSE, Sri Muthukumaran Institute of Technology, Chennai, India[2]
Professor, Department of CSE, Sri Muthukumaran Institute of Technology, Chennai, India[3]

Abstract: we present a novel automatic framework to perform 3D face recognition. The proposed method uses a Simulated Annealing-based approach (SA) for range image adjustment with the Surface Interpenetration Measure (SIM), as similarity measure, in order to match two face images. A modified SA approach is proposed taking advantage of constant face regions to better handle facial expressions. The authentication score is obtained by combining the SIM values corresponding to the matching of four different face regions: circular and elliptical areas around the nose, forehead and the entire face region. Comprehensive experiments were performed on the FRGC v2 database, the largest available database of 3D face images. By using all the images in the database, a verification rate of 96.5% was achieved at a False Acceptance Rate (FAR). The experiments simulated both verification and identification systems and the results compared to those reported by state-of-the-art works. In the identification scenario, rank-one accuracy was achieved. To the best of our knowledge, this is the highest rank-one score ever achieved for the FRGC v2 database when compared to results published in the literature.

Keywords: 3D Face Recognition, Surface Interpenetration Measure (SIM), Range Image Registration.

I. INTRODUCTION

FACE recognition is a very challenging subject. So far, studies in 2D face recognition have reached significant development, but still bear limitations mostly due to pose variation, illumination, and facial expression [13]. One way to overcome such limitations is the use of face depth information. In the 90's, 3D face recognition stood out due to advances of 3D imaging sensors. However, 3D images also have limitations, such as the presence of noise and difficult image acquisition [7]. A common approach for 3D face recognition is the use of registration techniques to perform range image matching. The Iterative Closest Point (ICP) [5] algorithm, or one of its variants, is usually sought to accomplish this task. The Mean Squared Error (MSE), minimized during the convergence process, is then used to compute the similarity between two face images [8], [9], [14], [17]. This approach can also be employed with deformation techniques to model facial expressions, minimizing its effects on face recognition [17], [19], [20].

The performance of both 2D and 3D face recognition systems can be verified on the Face Recognition Grand Challenge (FRGC) [14]. The FRGC is an international benchmarking composed of six challenging problems with its expected performance guidelines. The third experiment, i.e. ROC III, regards the 3D face recognition problem using a challenging database composed of 4,007 images from 466 subjects displaying different facial expressions. For this experiment, the goal is to achieve a verification rate of 98.0% at a False Acceptance Rate (FAR) of 0.1% [14].

Initially, the 3D face image can be acquired by different techniques, such as laser and structured light scanners [15]. In the preprocessing stage, the input image is smoothed and the face region is automatically detected and segmented. Then, some facial feature points are detected to be used during the matching process [11]. Each segmented face region is matched with its corresponding one in the database. A Simulated Annealing-based approach (SA) for range image registration runs the process by using two robust measures to assess alignment precision: (1) M-estimator Sample Consensus (MSAC) [37], and (2) Surface Interpenetration Measure (SIM) [11]. In previous works, the SIM showed to be a discriminatory measure when working on face images [4], [15].

This paper is organized as follows. Section II discusses the main related works. Section III presents details about the images available in the FRGC v2 database. Section IV describes the preprocessing stage. Section V regards the

ISSN 2394-3777 (Print)
ISSN 2394-3785 (Online)
Available online at www.ijartet.com

International Journal of Advanced Research Trends in Engineering and Technology (IJARTET)
Vol. 6, Issue 4, April 2019

proposed method for face image matching and Section VI regards the 3D face authentication process. Section VII presents the experimental results and Section VIII concludes with the final remarks.

II. Literature Review

Chang et al. [8] describe a method called Adaptive Rigid Multi-Region Selection (ARMS). ARMS uses three different overlapping regions around the nose: (a) circle, (b) ellipse, and (c) the nose itself. The nose region was designated because it is invariant in the presence of facial expression. Each region is matched with its corresponding one using ICP and the resulting Root Mean Square Error (RMSE) of each alignment is combined using the product rule. This value is then used as similarity measure between face images. Experiments were performed using the super set of images from the FRGC, composed of 4,485 3D face images. A rank-one accuracy of 97.1% was achieved when using a dataset composed of neutral images; and a rank-one accuracy of 87.1% when using a dataset containing faces with facial expression.

Kakadiaris et al. [19] present a fully automated framework for 3D face recognition using the Annotated Face Model (AFM) to overcome the facial expression problems. An AFM is previously created to be used during alignment and deformed in the matching stage, allowing the creation of a metadata for authentication. In earlier steps of the framework, the input image is processed for spike removal and holefilling. A subsample of the data is created to improve the method efficiency. Before the fitting procedure starts, the raw data is aligned to the AFM model using a multistage matching method which combines three matching procedures: (1) Spin Images, (2) ICP and (3) SA on Z-buffers. A deformed model is obtained after the fitting process and it is converted into a geometric model and a normal map. Each image is then treated separately using two wavelet transformations, Pyramid and Haar. Authentication is computed in wavelet domain by assessing a different distance metric for each wavelet type. In the ROC III experiment of the FRGC v2, they reported a verification rate of 97.0%, at 0.1% FAR. Also, they reported a rank one performance of 97.0%.

Faltemier et al. [14] develop a system that consists in the fusion of 28 spherical regions extracted from the face. These regions are then combined using the ICP algorithm. The distance obtained from the matching of each region was combined using different approaches, and the best results were reported using Consensus Voting and Borda Counting. To make the system more robust for small variations, which may occur in some face regions, different small regions are used for matching. Experiments on the FRGC v2 database achieved a verification rate of 93.2% at 0.1% FAR and a rank-one performance of 97.2%.

For a survey of works related to 3D and multimodal 2D+3D face recognition the reader should refer to [2], [7]. As observed in this section, most works successfully employ the ICP algorithm for 3D face recognition [8], [14], [17], [18]. Then, the MSE, sometimes combined with other measures, is used as the similarity score. In this paper we present a novel approach, applying the SIM to obtain more precise results.

III. 3D Face Image Database

The disturbance presented in (1) was caused because the subject moved during the acquisition process. The second problem regards the distance between the person and the acquiring system. If a person is too close, closer regions such as nose may not be properly scanned because of focal range limitations. Besides, the laser sensor cannot deal well with transparent regions and regions with high specularity, which causes holes in the scanned image, e.g., in the eyes and around the nose. Bowyer et al. [7] addressed this issue and identified several situations that affect range image quality, such as environment illumination. Some of these peculiarities from the FRGC v2 database have also been reported by Maurer et al. [17].

TABLE 1
FRGC v2 Face Image Classification.

Image sets	Number of images
Small expression with artifacts	247
Small expression without artifacts	455
Neutral without artifacts	933
Neutral with/without artifacts	2,182
All	4,007

ISSN 2394-3777 (Print)
ISSN 2394-3785 (Online)
Available online at www.ijartet.com

International Journal of Advanced Research Trends in Engineering and Technology (IJARTET)
Vol. 6, Issue 4, April 2019

Aiming the verification of the robustness of our approach for 3D face recognition, we manually classified the FRGC v2 database according to facial expression and noise level (regarding the artifacts). We performed a careful facial expression classification because the one provided by FRGC has some misclassified images. This probably occurred because the classification was made according to the prompting request, whereas an outside observer may assign a different label to the image. Fig. 1 shows examples of faces classified as neutral expression by FRGC, but those actually have facial expression. In this paper, the database is segmented into different sets of images as presented in Table 1.

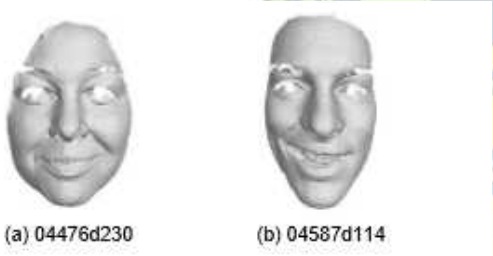

Fig.1.Example of images classified as neutral in FRGC v2 database

We classified the FRGC v2 database into three datasets according to holes in the eye region: (1) without holes, in 51 images, (2) small holes, in 1,300 images, and (3) large holes, in 2,656 images. This occurs because the eye is translucent and the light stripe is refracted instead of being reflected. Due to this, the laser scanner cannot properly capture a reflection and then no information is produced in this region. We noticed that almost all the images from the database presented artifacts. Because of this, we do not consider the eye holes as a disturbance.

IV. 3D Face Image Preprocessing

After the face region is segmented, six feature points are detected to extract rigid regions of the face and improve the matching process; the inner right and left eye corners, the right and left nose corners, the nose tip and base, as shown in Fig. 1a. To perform this task we use our own approach that is able to detect automatically the eye corners and the nose features (i.e. tip, corners and base) in 99.92% and 99.6% of the images from FRGC v2, respectively. The nose features were not correctly detected due to nose absence only in three images (see Fig. 1b). The eye corners could not be correctly detected in 16 images due to the head pose rotation (see Fig 2c). In our experiments we used the points as they were detected. However, these images had minor negative impact in our results due to our hierarchical approach that uses different regions. Further details are presented in [15].

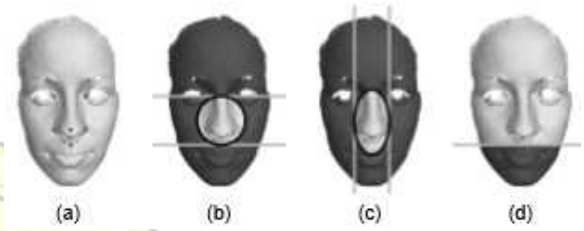

Fig.2.Segmented regions from a same face: (a) entire face and detected feature points, (b) circular nose area, (c) elliptical nose area and (d) upper head.

In [4] it is stated that, when using the SIM, the nose region alone is not enough discriminatory for face recognition because it represents only a small fraction of the face; therefore, regions (3) and (4) were also used because they have more information about the face. Region (3) is obtained by selecting all face points above the nose base point, as shown in Fig. 2d. Therefore, the four segmented regions are used to perform face recognition.

V. 3D Face Matching

In the present work we use the SA to perform the range image matching using two robust measures: (1) MSAC [18], and (2) SIM. The SA starts the registration process using the MSAC and the final tuning is achieved by using the SIM. The resulting SIM value is then used to assess the final 3D face matching. The following sections present a brief explanation regarding the SIM and SA.

5.1 Surface Interpenetration Measure (SIM)

Through the quantification of interpenetration, one can more precisely assess the registration results and provide a highly robust control. Registrations of two range images presenting good interpenetration have high SIM values, and erroneous alignments produce low SIM values and those small differences in MSE can yield significant differences in SIM. Furthermore, alignments with high SIM present a very low interpoint distance between the two surfaces. That is, SIM is a far more sensitive indicator of alignment quality when comparing “reasonable” alignments.

ISSN 2394-3777 (Print)
ISSN 2394-3785 (Online)
Available online at www.ijartet.com

International Journal of Advanced Research Trends in Engineering and Technology (IJARTET)
Vol. 6, Issue 4, April 2019

5.2 SA approach for range image registration

The Simulated Annealing (SA) [20] is a stochastic algorithm for local search. From an initial candidate solution, SA iteratively searches a better neighbor solution to the problem as compared to the current one. The main difference between SA and other local search algorithms, e.g. Hill Climbing, is that SA can accept a worse solution than the current candidate during the iterative process; therefore, SA does not remain "tied" to local minima and because of this it has higher chances to reach its goal, which is a solution close enough to the global one.

Algorithm 1 Surface Interpenetration Measure – SIM.

Require: Two range images A and B
1: **for** $p \in A$ **do**
2: Define a $n \times n$ neighborhood N_p centered in p;
3: Search the corresponding point e of p in B, with $e \notin D$;
4: Compute angle θ between normal vectors $\vec{n_p}$ and $\vec{n_e}$, regarding points p and e;
5: **if** $\theta < m$ **then**
6: **for** $q_i, q_j \subset N_p$, with $q_i \neq q_j$ **do**
7: **if** $[(q_i \quad e) \cdot n'_e] \cdot [(q_j \quad e) \cdot n'_e] < 0$ **then**
8: $C_{(A,B)} \leftarrow C_{(A,B)} \bigcup p$;
9: **end if**
10: **end for**
11: **end if**
12: **end for**
13: **return** $\frac{C_{(A,B)}}{|A|}$

The SA method requires the modeling of the problem in such a way that it is possible to move from a candidate solution to any neighbor one. For registration of two range images, six parameters (regarding rotation and translation on X, Y and Z axis, respectively) are defined as a "transformation vector". When applying this vector to one image, it is possible to align it with another one.

VI. 3D Face Authentication

To accomplish 3D face authentication we used the SIM scores computed by matching segmented facial regions. If two face images are from the same person, the matching produces a high SIM value; otherwise, it computes a low SIM value. We performed one first experiment to verify which region produced the best result for face recognition. Table 2 shows verification results using only each region. The first column describes the face region used, followed by the verification rate. The last column presents the number of false rejections, i.e., number of combinations from the same subjects that were rejected.

TABLE 2
Verification rate for each face region, at 0% FAR.

Regions	Verification Rate	False Rej.
Nose circle (C)	87.4%	627
Nose ellipse (E)	89.6%	519
Upper head (U)	85.0%	749
Face region (F)	89.6%	516
Face using modified SA (M)	87.3%	631

By observing these results, the upper head region presented the highest verification rate mainly because the mouth, which is largely affected by expressions, was removed. Results show that the modified SA procedure presented inferior results when compared to the original SA approach. However, in [22] we stated that modified SA was more suitable when comparing neutral face images to others with expression; and an improvement of 15% was reported over original SA approach. Then, we performed a second experiment, in which we combined scores for each region using the sum rule. The value obtained from the sum is then used as similarity score for two faces.

VII. Experimental Results

Experiments were performed intending to reproduce a genuine face recognition system, where matching is performed between an acquired face image with others stored in a database. The experiments assessed two types of authentication systems: verification and identification. In verification systems, the objective is to answer if a person is who he/she claims to be. The performance is measured assessing the verification rate achieved at a predefined FAR. When using a 0% FAR, it is possible to ensure that any non-authorized person is going to be accepted in the authentication system. Identification systems retrieve the identity of a person comparing the input image with the entire database. The system outputs a rank of the most similar faces based on similarity score. Performance is measured using rank-one accuracy, which indicates when the best matching score is actually from the same subjects [6]

ISSN 2394-3777 (Print)
ISSN 2394-3785 (Online)
Available online at www.ijartet.com

International Journal of Advanced Research Trends in Engineering and Technology (IJARTET)
Vol. 6, Issue 4, April 2019

7.1 SA-Based Approach Performance

The time constraint is one of the main worries when using SA to perform 3D face matching in an authentication system. We performed an experiment using a controlled environment for time analysis. A set of 200 random images were selected and combined with each other, totaling 19,900 combinations. We used a computer with the following configuration: Linux O.S., Intel Pentium D 3.4GHz, cache of 2MB and 1GB of memory. Table 3 presents the average execution time of the SA approach regarding the matching of two face regions.

TABLE 3

Average time performance using SA for face matching.

Regions	Average time
Nose circle	1.5s
Nose ellipse	1.2s
Upper head	2.0s
Face region	3.2s
Face using modified SA	3.1s

7.2 Experiment I: Verification

In this experiment we defined a controlled dataset as gallery and the other ones as probe. Each image from the probe dataset was compared with the ones presented in gallery. Results are presented in Table 4. The first two columns are the gallery and probe datasets used in experiment, respectively. The third column is the verification rate at 0% FAR, followed by the number of false rejections FR. Last two columns show the verification rate at 0.1% FAR and number of false rejections FR, respectively.

TABLE 4

Experiment I: Verification rate using 0%and 0.1% FAR.

Gallery	Probe	FAR 0%	FR	FAR 0.1%	FR
Level 0	Level 0	99.2%	39	100.0%	0
Level 0	Level 1	98.9%	71	99.9%	3
Level 0	Level 2	97.2%	216	99.8%	18
Level 0	Level 3	96.5%	294	99.7%	29
Level 0	All	90.7%	1,067	98.5%	175
Level 1	All	83.5%	4,312	98.2%	475
All	All	70.7%	13,736	96.5%	1,648

The experimental results analysis show that when faces with expression and artifacts are added to the datasets, the verification rate is considerably affected on both 0% FAR and 0.1% FAR. This behavior is expected since we perform matching assuming that the face is a rigid object. Results from Table 4 differ from the ones presented in [22] because we changed the SA parameters aiming to reduce its computational time.

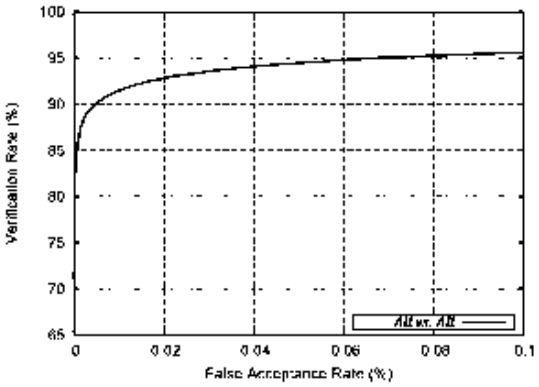

Fig. 3. System performance for "All vs. All" experiment

We also performed the "All vs. All" experiment, where every image of FRGC v2 is matched with all remaining others. It resulted 16,052,042 combinations, from which 46,920 were comparisons from same subjects. In this experiment a 95.6% authentication rate was achieved at 0.1% FAR. Fig. 3 presents the corresponding FAR curve for this experiment.

7.3 Experiment II: Identification

For the identification experiment, we defined probe and gallery datasets. In this experiment, we defined four datasets as gallery: (1) Level 0, with 933 images, (2) Level 1, with the 2,182 images, (3) First with 465 images corresponding to the first image from each subject that appears into the database, and (4) All, with 4,007 images. The probe dataset for each gallery includes all the remaining images from the database which are not in the gallery dataset. From the probe dataset, only the subjects with a corresponding image in the gallery were evaluated. For the experiment using All dataset, each subject from probe was compared with the other 4,006 remaining ones stored in the database. The Cumulative Match Curve (CMC) is presented in Fig. 4 and results achieved for rank-one are presented in Table 5.

ISSN 2394-3777 (Print)
ISSN 2394-3785 (Online)
Available online at www.ijartet.com

International Journal of Advanced Research Trends in Engineering and Technology (IJARTET)
Vol. 6, Issue 4, April 2019

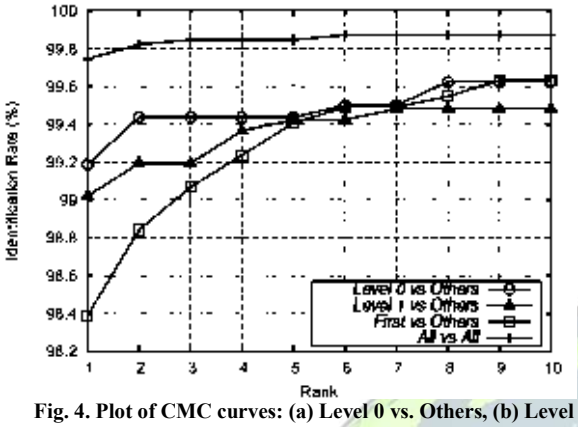

Fig. 4. Plot of CMC curves: (a) Level 0 vs. Others, (b) Level 1 vs. Others, (c) First vs. Others, and (d) All vs. All

By observing the experimental results, the proposed approach achieved rank-one recognition higher than 98%. The experiment all vs. all presented the highest recognition rate, because one subject may have more than one image stored into the gallery dataset. In fact, Faltemier et al. [13] show that by using a gallery composed of multiple images it is possible to obtain higher performance.

TABLE 5

Experiment II: Rank-one recognition rate.

Gallery	Probe	Rank-one	False Rej.
Level 0	*Others*	99.2%	13
Level 1	*Others*	99.0%	17
First	*Others*	98.4%	57
All	*All*	99.7%	10

VIII. FINAL REMARKS

We performed extensive experiments on the FRGC v2 database to evaluate the performance of our method. The database was manually segmented into different datasets according to the images facial expression intensity and noise level. Then we made an accurate analysis regarding our method behavior. We also detected a subject with two different identities in the database with this analysis. By using this novel approach one can distinguish whether two face images with neutral expression belong to the same subject or not with a verification rate of 99%, at 0% FAR. From the experimental results we observed that, when comparing a neutral face with other faces with expressions, the performance of our method slightly decreases. When using all images in the database, in the "All vs. All" experiment, faces still can be recognized with 96.5% accuracy, at 0.1% FAR. In an identification scenario, our method achieves a 98.4% recognition rate when using the "First vs. Others" dataset. Also, for all the experiments performed in the identification mode, our method achieved rank-one accuracy greater than 98%. To the best of our knowledge, these are the best results for this experiment reported in the literature.

We also developed an extended approach of the hierarchical evaluation method to perform a verification experiment at 0% FAR [12]. By including partial sum rules during hierarchy analysis, we improved the verification rate from 70.7% to 77.5%, in the "All vs. All" experiment. In the FRGC ROC III experiment, we achieved a verification rate of 96.6%, at 0.1% FAR, and a rank-one accuracy of 98.3%. Although our method is affected when images contain facial expression and artifacts, we obtained results very close to the one reported by Kakadiaris et al. [19], which employs deformable face models to deal with the facial expressions. Moreover, we performed an experiment to verify whether the recognition rate could be improved if the time constraint is avoided. The SA matching was performed using a larger number of iterations, and the results improved the recognition rate. With this, we show the potential of the SIM as similarity score for 3D face recognition.

REFERENCES

[1]. "IMAGO Research Group: 3D face recognition homepage," http://www.imago.ufpr.br/3D Face Recognition.

[2]. F. Al-Osaimi, M. Bennamoun, and A. Mian, "An expression deformation approach to non-rigid 3D face recognition," Int'l Journal of Computer Vision, p. Online first, September, 2008.

[3]. P. J. Besl and N. D. McKay, "A method for registration of 3-D shapes," IEEE Trans. Pattern Anal. Mach. Intell., vol. 14, no. 2, pp. 239–256, 1992.

[4]. A. F. Abate, M. Nappi, D. Riccio, and G. Sabatino, "2D and 3D face recognition: A survey," Pattern Recognition Letters, vol. 28, no. 14, pp. 1885–1906, 2007.

[5]. K. W. Bowyer, K. Chang, and P. J. Flynn, "A survey of approaches and challenges in 3D and multi-modal 3D+2D face recognition," Computer Vision and Image Understanding, vol. 101, pp. 1–15, 2006.

ISSN 2394-3777 (Print)
ISSN 2394-3785 (Online)
Available online at www.ijartet.com

International Journal of Advanced Research Trends in Engineering and Technology (IJARTET)
Vol. 6, Issue 4, April 2019

[6]. J. Cook, V. Chandran, S. Sridharan, and C. Fookes, "Face recognition from 3d data using iterative closest point algorithm and gaussian mixture models," in Proc. Int'l Symposium 3D Data Processing, Visualization and Transmission, 2004, pp. 502–509.

[7]. S. Drovetto Jr., L. Silva, and O. R. P. Bellon, "Hierarchical evaluation model for 3D face recognition," in Proc. Int'l Conf. Computer Vision Theory and Applications, vol. 2, 2008, pp. 67–74.

[8]. J. Cook, C. McCool, V. Chandran, and S. Sridharan, "Combined 2D/3D face recognition using log-gabor templates," in Proc. IEEE Int'l Conf. Video and Signal Based Surveillance, 2006, p. 83.

[9]. P. J. Flynn, T. Faltemier, and K. W. Bowyer, "3D face recognition," in Handbook of Biometrics, A. K. Jain, A. Ross, and P. J. Flynn, Eds. Springer, 2008, ch. 11, pp. 211–229.

[10]. G. Dalley and P. J. Flynn, "Range image registration: A software platform and empirical evaluation," in Proc. Int'l Conf. 3-D Digital Imaging and Modeling, 2001, pp. 246–253

[11]. M. Husken, M. Brauckmann, S. Gehlen, and C. V. der Malsburg, "Strategies and benefits of fusion of 2D and 3D face recognition," in Proc. IEEE Conf. Computer Vision and Pattern Recognition. IEEE Computer Society, 2005, pp. 174–174.

[12]. S. Kirkpatrick, C. D. Gelatt, and M. P. Vecchi, "Optimization by simulated annealing," Science, vol. 220, no. 4598, pp. 671–680, 1983.

[13]. I. Kakadiaris, G. Passalis, G. Toderici, N. Murtuza, and T. Theoharis, "Three-dimensional face recognition in the presence of facial expression: An annotated deformable model approach," IEEE Trans. Pattern Anal. Mach. Intell., vol. 29, no. 4, pp. 640–649, 2007.

[14]. W.-Y. Lin, K.-C. Wong, N. Boston, and Y. H. Hu, "3d face recognition under expression variations using similarity metrics fusion," in Proc. IEEE Int'l Conf. Multimedia and Expo, 2007, pp. 727–730.

[15]. X. Lu, A. K. Jain, and D. Colbry, "Matching 2.5D face scans to 3D models," IEEE Trans. Pattern Anal. Mach. Intell., vol. 28, no. 1, pp. 31–43, 2006.

[16]. M. Lundy and A. Mees, "Convergence of an annealing algorithm," Mathematical Programming: Series A and B, vol. 34, no. 1, pp. 111–124, 1986.

[17]. T. Maurer, D. Guigonis, I. Maslov, B. Pesenti, A. Tsaregorodtsev, D. West, and G. Medioni, "Performance of geometrix activeid 3D face recognition engine on the FRGC data," in Proc. IEEE Conf. Computer Vision and Pattern Recognition. IEEE Computer Society, 2005, pp. 154–154.

[18]. J. Kittler, M. Hatef, R. Duin, and J. Matas, "On combining classifiers," IEEE Trans. Pattern Anal. Mach. Intell., vol. 20, no. 3, pp. 226–239, 1998.

[19]. A. Mian, M. Bennamoun, and R. Owens, "An efficient multimodal 2D-3D hybrid approach to automatic face recognition," IEEE Trans. Pattern Anal. Mach. Intell., vol. 29, no. 11, pp. 1927–1943, 2007.

[20]. W.-Y. Lin, K.-C. Wong, N. Boston, and Y. H. Hu, "3d face recognition under expression variations using similarity metrics fusion," in Proc. IEEE Int'l Conf. Multimedia and Expo, 2007, pp. 727–730.

[21]. A. Mian, M. Bennamoun, and R. Owens, "An efficient multimodal 2D-3D hybrid approach to automatic face recognition," IEEE Trans. Pattern Anal. Mach. Intell., vol. 29, no. 11, pp. 1927–1943, 2007.

[22]. A. Martinez, "Recognizing imprecisely localized, partially occluded, and expression variant faces from a single sample per class," IEEE Trans. Pattern Anal. Mach. Intell., vol. 24, no. 6, pp. 748–763, Jun 2002.